Chin. J. Chem. Eng., **15**(1) 75—80 (2007)

Multiobjective Optimization of the Industrial Naphtha Catalytic Reforming Process*

HOU Weifeng(侯卫锋)**, SU Hongye**(苏宏业)****, MU Shengjing**(牟盛静) **and CHU Jian**(褚健)
National Laboratory of Industrial Control Technology, Institute of Advanced Process Control, Zhejiang University, Hangzhou 310027, China

Abstract In this article, a multiobjective optimization strategy for an industrial naphtha continuous catalytic reforming process that aims to obtain aromatic products is proposed. The process model is based on a 20-lumped kinetics reaction network and has been proved to be quite effective in terms of industrial application. The primary objectives include maximization of yield of the aromatics and minimization of the yield of heavy aromatics. Four reactor inlet temperatures, reaction pressure, and hydrogen-to-oil molar ratio are selected as the decision variables. A genetic algorithm, which is proposed by the authors and named as the neighborhood and archived genetic algorithm (NAGA), is applied to solve this multiobjective optimization problem. The relations between each decision variable and the two objectives are also proposed and used for choosing a suitable solution from the obtained Pareto set.
Keywords multiobjective optimization, catalytic reforming, lumped kinetics model, neighborhood and archived genetic algorithm (NAGA)

1 INTRODUCTION

Petroleum refining and petrochemical industries aim at maximizing one prime product while simultaneously minimizing another accessory product to improve the quality of the prime product. Unfortunately, the two requirements are often conflicting or inconsistent. It is necessary to determine the trade-off compromises to balance the two objectives[1,2].

As the core of aromatics complex unit, catalytic reforming is a very important process for transforming naphtha into aromatics feedstock[3]. In this process, the yield of aromatics, including benzene, toluene, para-xylene, meta-xylene, ortho-xylene, ethyl-benzene, and heavy aromatics (*i.e.* 9 and more carbon aromatics), are regarded as the main index that determines the quality. However, heavier aromatics are not required and will increase the load on the downstream units of the aromatics complex process, especially on the disproportionation and xylene fractionation units. Thus, the design and operation of the catalytic reforming process require multiobjective optimization to balance the various objective functions.

Multiobjective optimization, involving more than one objective function, was typically modeled and solved by transforming it into a single objective problem using different methods, such as the restriction method, the ideal point method, and the linear weighted sum method. These methods largely depend on the values assigned to the weighted factors or the penalties used, which are done quite arbitrarily. Another disadvantage of the above methods is that these algorithms obtain only one optimal solution at a time and may miss some useful information[4].

Recently, multiobjective evolutionary algori-thms are used more popularly in industrial process modeling, optimal design, and operation[4]. These may produce a solution set, which is named as a Pareto set, in a single run of the algorithms. The Pareto solutions are extremely useful in industrial operations as these narrow down the choices and help to guide a decision-maker in selecting a desired operating point (called the preferred solution) among the (restricted) set of Pareto optimal points, rather than from considerably large number of possibilities[5]. Coello[6] presented comprehensive reviews on the development of the evolutionary (especially genetic) multiobjective optimization. When compared with the previous methods, such as the nondominated sorting genetic algorithm (NSGA)[7], the niched Pareto genetic algorithm (NPGA)[8], the Pareto archive evolutionary strategy (PAES)[9], and the strength Pareto evolutionary algorithm (SPEA)[10], the method employed in this study, the neighborhood and archived genetic algorithm (NAGA)[11,12], offers several advantages: (1) low computation complexity; (2) insensitivity of the efficiency to the method parameters; and (3) uniform distribution on the Pareto front.

In this article, the multiobjective optimization strategy for an industrial naphtha continuous catalytic reforming process is built to improve the operation level. A 20-lumped kinetic model is employed for the industrial catalytic reforming reaction and the corresponding process model is validated by successful industrial applications[13]. In the catalytic reforming unit, the objectives are to maximize the aromatics yield and minimize the yield of heavy aromatics. The multiple Pareto optimal solutions of the problem are obtained by applying the multiobjective genetic algorithm, NAGA. It presents an operating parameter set for operators for various operational targets.

2 DESCRIPTION OF THE PROCESS AND MODELING

The simplified continuous catalytic reforming process flow diagram is shown in Fig.1. The naphtha, used as the catalytic reformer feedstock usually

Received 2005-11-19, accepted 2006-07-03.
* Supported by the National Natural Science Foundation of China (No.60421002).
** To whom correspondence should be addressed. E-mail: hysu@iipc.zju.edu.cn

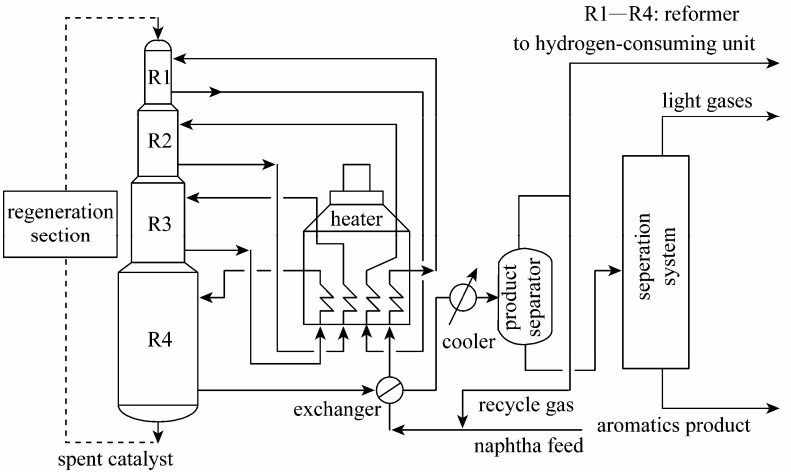

Figure 1 Flowsheet of a continuous catalytic reforming process

containing more than 300 chemical compounds of paraffins, naphthenes, and aromatics in the carbon number range of C_4 to C_{12}, is combined with a recycle gas stream containing 60% to 90% (by mol) hydrogen. The total reactor charge is heated and passed through the catalytic reformers, which are designed with four adiabatically operated reactors and four heaters between the reactors to maintain the reaction temperatures at design levels. The effluent from the last reactor is cooled, which then enters the product separator. The flashed vapor circulates to join the naphtha feedstock as recycle gas. Excess hydrogen from the separator is sent to other hydrogen-consuming units. The separated liquid that chiefly comprised the desired aromatics together with light gases and heavy paraffins is sent to the separation system to obtain aromatics products.

The aromatics products are obtained by the conversion of *n*-paraffins and naphthenes in naphtha to iosparaffins and aromatics over bifunctional catalysts such as Pt-Sn/Al_2O_3 in the four reactors. The dominant reaction types of catalytic reforming are dehydrogenation of naphthenes, isomerization of paraffins and naphthenes, dehydrocyclization of paraffins, hydrocracking of paraffins, and hydro-dealkylation of aromatics. Dehydrogenation is the fastest reaction followed by isomerization, which is moderately fast, whereas dehydrocyclization and hydrocracking are the slowest.

As mentioned above, the naphtha feedstock is very complex and each of these undergoes various reactions. To reduce the complexity of the model to a manageable level, the large number of naphtha components are assigned to a smaller set of kinetics lumps, each of which is composed of chemical species that are grouped together according to some criteria[14]. Accordingly, various lumped kinetics models with varying levels of sophistication that represent catalytic reforming reactions have been reported in the literature[15—20].

In the previous study[13], a simple lumped kinetics model for catalytic reforming with 20 lumps involving 31 reactions was presented. The corresponding reaction network is shown in Fig.2. In this model, the total reactor charge is characterized as paraffins (P), naphthenes (N), and aromatics (A) lumps with the carbon number ranging from 6 to 9+(9+indicates a carbon number of 9 and above) and light paraffins (P_1—P_5), in which the 8-carbon aromatics are subdivided into their four isomeric compounds, *i.e.* PX (para-xylene), MX (meta-xylene), OX (ortho-xylene), and EB (ethyl-benzene). The rationale of selecting these lumps was based on both thermodynamic and kinetics considerations for the aromatization selectivity of paraffins and naphthenes. It is not necessary to split the paraffin or naphthene lumps into their individual isomers (*e.g.*, isohexane and *n*-hexane) for achieving similar aromatization selectivity for the two lumps (except for methyl cyclopentane and hexane) and for faster isomerization reaction rates relative to dehydrocyclization and hydrocracking[15,16]. In this reaction network, except for isomerization, all the dominant catalytic reforming reactions are included.

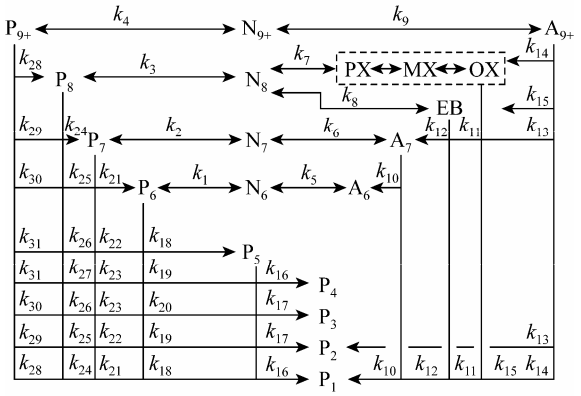

Figure 2 Reaction scheme for naphtha reforming

All the 31 rate equations are nonlinear pseudo-monomolecular in nature, with the rate coefficients obeying the Arrhenius law, as shown in Eq.(1),

$$k_j = k_{0j} \cdot \exp\left(-E_j / RT\right) \cdot P_h^{\theta_j} \cdot \phi$$
$$0 < \phi \leqslant 1,\ j=1—31 \qquad (1)$$

Under the normal reformer operating conditions, radial and axial dispersion effects were found to be negligible[13]. For the radial flow reactor, the global material and the heat balance equations are given in Eqs.(2) and (3), respectively,

$$\frac{\mathrm{d}\boldsymbol{Y}}{\mathrm{d}R}=\frac{2\pi R\cdot H}{(\mathrm{LHSV}\cdot V_{\mathrm{c}})}\cdot K_{\mathrm{r}}\cdot\boldsymbol{Y} \tag{2}$$

$$\frac{\mathrm{d}T}{\mathrm{d}R}=\frac{2\pi R\cdot H}{(\mathrm{LHSV}\cdot V_{\mathrm{c}})}\cdot\sum_{j=1}^{31}\frac{\left(r_j\cdot\Delta H_j\right)}{\left(\boldsymbol{C}_p\cdot\boldsymbol{Y}\right)} \tag{3}$$

where $\boldsymbol{Y}$ is the vector of the molar flow rates including 20 lumps and H_2. Eq.(2) is solved using a mixed numerical algorithm of fourth-order Runge-Kutta and Gear method, and Eq.(3) is solved using the modified Euler method. The thermochemical properties of each lump are computed by taking an arithmetic average of the properties of the corresponding pure chemical components constituting the lump.

The product separator was modeled to perform in isothermal flash operation. A Peng-Robinson equation was used to compute the vapor/liquid equilibrium constants. The so-called sequential modular approach is implemented for the computation of this flowsheet. Except for the separation system, the reactors, the heaters, the product separator, and the heat exchangers are included in this computation.

If the activation energies (E), the pressure exponents (θ), and the frequency factors (k_0) for all 31 reactions are estimated, there will be 93 kinetics parameters in total, and it is very difficult to determine these parameters synchronously. Generally, E and θ values reported by different literatures for the specific catalyst are similar. To reduce the difficulty experienced in estimating parameters, the parameters E and θ in this model are taken from Ref.[18] and only thirty-one k_0, which considers the difference between the estimation of parameters E and θ, and the unmodeled kinetics, are estimated.

The procedure of parameter estimation is carried out by minimization of the sum of the squares of the deviations between the plant and the calculated values of the key variables such as the compositions of effluent from the last reactor and the outlet temperatures of the four reactors. The operating and assaying data samples of several months for the industrial process, which are first reconciled by material balance, are used to estimate k_0 by the BFGS optimization algorithm.

3 FORMULATION OF THE OPTIMIZATION PROBLEM

The variables that affect the catalytic reforming process are the volume flow of naphtha charge to the volume of the catalyst (liquid hourly space velocity, LHSV), the latent aromatics content of naphtha charge (LA), the four reactor inlet temperatures (T_1, T_2, T_3, T_4), the reaction pressure (p_{r}), the mole flow of hydrogen in the recycle gas to the mole flow of naphtha charge (hydrogen-to-oil molar ratio, $n_{\mathrm{H_2}}/n_{\mathrm{HC}}$), the product separator temperature (T_{s}), *etc*.. Among the 9 process variables selected using mechanism analysis, the sensitivity analysis of each variable is performed using the process model presented in Section 2 to obtain its quantitative corrections with the aromatics yield and the yield of heavy aromatics. It is shown that the appropriate set point value of one variable for maximizing the aromatics yield may not be suitable for minimizing the yield of heavy aromatics. Therefore, the suitable trade-off solutions for the two optimal objectives should be considered.

For the continuous catalytic reforming process in this study, the unit is in full load operation and the value of LHSV cannot be further increased. Similarly, the quality of naphtha feedstock (*e.g*. LA) cannot be changed artificially for most domestic petroleum-refining enterprises. The product separator temperature T_{s} is not independent of other variables. Moreover, for further lowering of the temperature, coolers need to be included in the system, which in turn increase the operation costs. Hence, the remaining process variables are selected as the decision variables for optimization in this study. These are the four reactor inlet temperatures (T_1, T_2, T_3, T_4), the reaction pressure (p_{r}), and the hydrogen-to-oil molar ratio ($n_{\mathrm{H_2}}/n_{\mathrm{HC}}$).

Thus, the two independent objectives, namely, the maximization of the aromatics yield (AY) and the minimization of the yield of heavy aromatics (HAY) are formulated mathematically as follows:

$$\begin{aligned}
&\text{maximize}\quad \mathrm{AY}(T_1, T_2, T_3, T_4, p_{\mathrm{r}}, n_{\mathrm{H_2}}/n_{\mathrm{HC}})\\
&\text{minimize}\quad \mathrm{HAY}(T_1, T_2, T_3, T_4, p_{\mathrm{r}}, n_{\mathrm{H_2}}/n_{\mathrm{HC}})\\
&\text{subject to}\\
&\qquad 520\leqslant T_1, T_2, T_3, T_4\leqslant 530\\
&\qquad 0.8\leqslant p_{\mathrm{r}}\leqslant 0.9\\
&\qquad 3.0\leqslant n_{\mathrm{H_2}}/n_{\mathrm{HC}}\leqslant 4.0\\
&\qquad 65\leqslant \mathrm{AY}\leqslant 68\\
&\qquad 18\leqslant \mathrm{HAY}\leqslant 23
\end{aligned} \tag{4}$$

The bounds of the decision variables and the objectives have been chosen based on industrial practice.

Because NAGA deals with only the minimization objective[11], the maximization of AY can be replaced by the minimization of a function f_1, where f_1=1/AY, without the replacement changing the location of the optima. To normalize the objective functions, the function f_1 is transformed to $f_1=K_{\mathrm{f}}/\mathrm{AY}$, and the function f_2 may be simplified as $f_2=\mathrm{HAY}/K_{\mathrm{c}}$, where K_{f}=67 and K_{c}=20 are the reference operating values of the aromatics yield and the yield of heavy aromatics, respectively.

4 RESULTS AND DISCUSSION

The solution for the multiobjective optimization problem described in Section 3 is obtained using NAGA. Table 1 provides the parameters of NAGA applied in this study.

Figure 3 shows the typical optimal solutions obtained by a single run of NAGA for the above formulated problem. The top of Fig.3 denotes the relationship

Table 1 Algorithm parameters used in this study

Parameters	Values
volume of the archive	100
maximum generation	500
probability of crossover	0.8
probability of mutation	0.01
population size	50
neighborhood size	0.05

between the two minimum objectives, f_1 *vs*. f_2, whereas the bottom depicts the solutions of the two original objectives. The conflict between the effects of the decision variables on the two objective functions, results in the optimum being a Pareto-optimal set rather than a unique solution. The Pareto set has the property that when one point on the set is moved to another, one objective function is improved (*e.g*. the aromatics yield increases), but the other function becomes worse (*e.g*. the yield of heavy aromatics increases accordingly). Hence, within the Pareto set, neither the solution dominates an over the other, and both indicate the optimal solation for the two objective functions and the minimization of the yield of heavy aromatics with the given operating bound. The operators have to use the additional information, such as the market quotation, the operating cost, and the corresponding decision variable values to select an operating point (preferred solution) from the entire Pareto set for operation.

Each point in Fig.3 represents a Pareto solution, which is associated with a set of the six decision variables. Fig.4 is a plot of the decision variables corresponding to each of the points on the Pareto set. Obviously, the relations between each decision variable and the two objectives can also be observed. Among the six variables, T_4 is unique in that all its points are close to its upper bound, which indicates that increasing T_4 results in both an increase in the aromatics yield and a decrease in the yield of heavy aromatics. However, increasing the decision variables T_1, T_2, p_r and n_{H_2}/n_{HC} results in a decrease in the yield of heavy aromatics, but a decrease in the aromatics yield. In other words, the four variables have opposing effects on the two minimum objectives f_1 and f_2. Besides the effects of the above variables, it is observed that the effects of T_3 on the two objective functions are mild.

All the above phenomena are confirmed by the process operators. These can also be rationally explained by the reaction mechanism. In the first and second reactors, the inlet temperature of 520℃ is adequate for the complete conversion of naphthenes to aromatics. A higher temperature is suitable for hydrocracking of paraffins, which results in the decrease of aromatics. In the fourth reactors, dehydrocyclization and hydrocracking of paraffins are the major reactions and are both aided by higher temperatures. In this study, the competition is more favorable for dehydrogenation and results in an obvious increase in aromatics. In any reactor, exothermic hydrodealkylation of aromatics increases with an increase of temperature, which indicates a decrease of heavy aromatics. On the other hand, lower pressure favors dehydrocyclization and dehydrogenation, but not hydrocracking and hydrodealkylation, which result in increase of both gross aromatics and heavy aromatics. Less n_{H_2}/n_{HC} indicates low partial pressure of hydrogen. Hence, n_{H_2}/n_{HC} and p_r have similar effects on the two objectives.

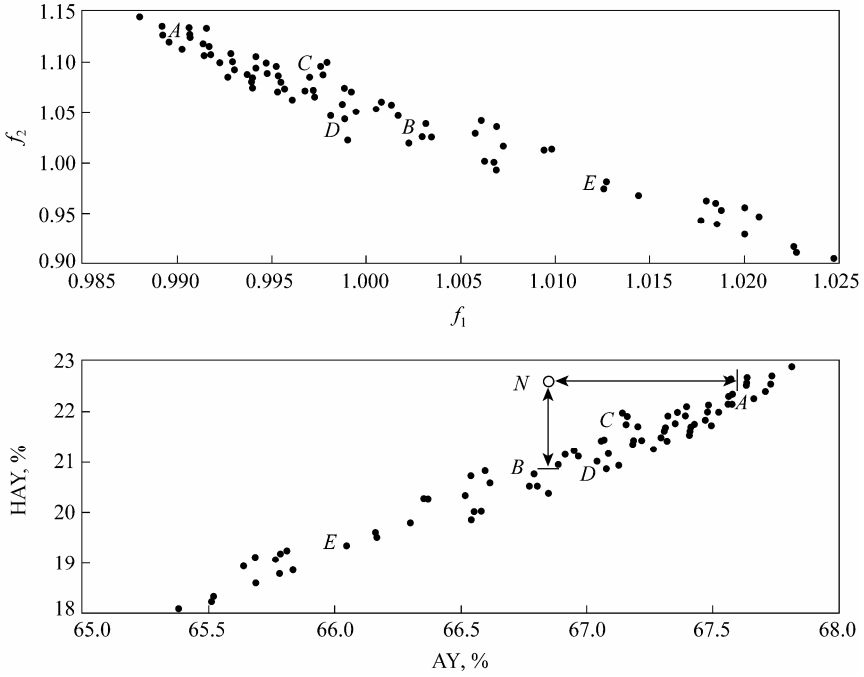

Figure 3 Pareto-optimal set of solutions obtained from the simultaneous optimization in f_1 *vs*. f_2 and in the original objectives of the aromatics yield and the yield of heavy aromatics

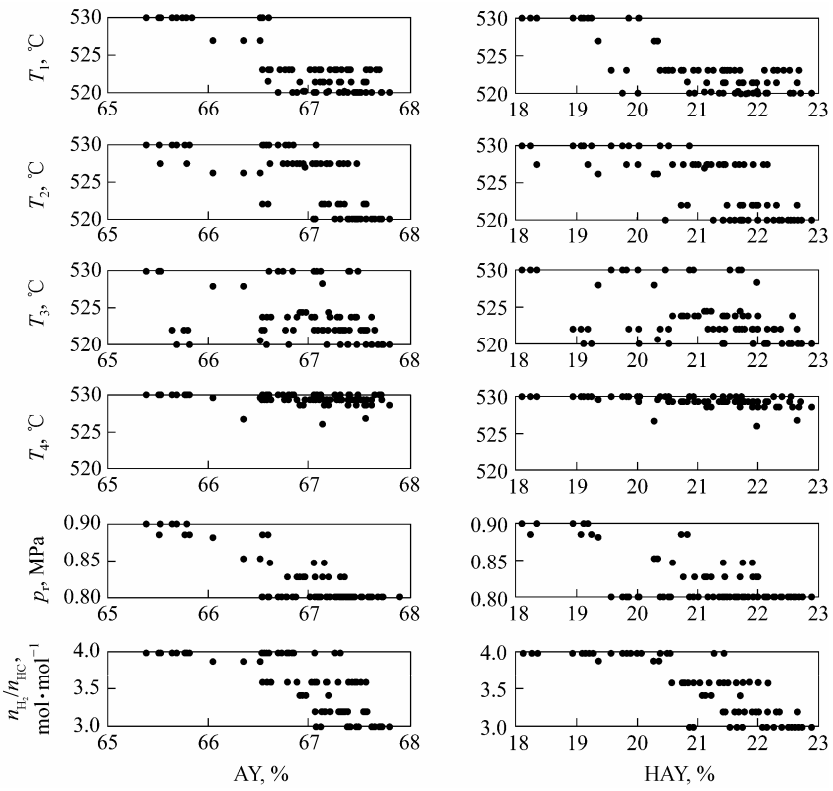

Figure 4 The decision variables corresponding to each of the Pareto-optimal solutions shown in Fig.3

The above relations between each decision variable and the two objectives are useful for selecting a suitable solution from the entire Pareto set. For example, the decision variable values and the corresponding objectives of several typical solutions, points *A*, *B*, *C*, *D*, and *E* in Fig.3, are listed in detail in Table 2. The point *N* denotes the industrial normal operating point, which is above the Pareto solution front that is obtained. If the aim is to increase the aromatics yield, it may be feasible to increase T_4 and (or) decrease p_r and n_{H_2}/n_{HC}, as listed in point *A* or *C*. While aiming to decrease the yield of heavy aromatics, it may be feasible to increase T_1, T_2, T_4, and (or) increase p_r and n_{H_2}/n_{HC}, as listed in point *B* or *E*. In actual industrial operations, p_r and n_{H_2}/n_{HC} are always maintained at higher values to protect the catalyst from rapid coking. As a solution to the above-mentioned problem, when other decision variables are approximately constant, only increasing T_4 by about 5℃ can lead to beneficial effects, an increase of 0.18% (by mass) in the aromatics yield and a decrease of 1.77% (by mass) in the yield of heavy aromatics, as listed in point *D*. The law that the increase of aromatics yield can only be obtained by slightly increasing T_4 has been validated in the same industrial continuous catalytic reforming unit, as reported in the previous literature[21].

5 CONCLUSIONS

The real-life challenge of promoting added value in the industrial naphtha continuous catalytic reforming process is described in this article. A 20-lumped kinetics model for catalytic reforming is used to solve the multiobjective optimization problem: maximization of the aromatics yield and simultaneous minimization of the yield of heavy aromatics. By performing the optimization based on the neighborhood and

Table 2 Comparison of the decision variables and objectives for normal operation and five possible cases of optimal operations

Points	Parameters							
	T_1, ℃	T_2, ℃	T_3, ℃	T_4, ℃	p_r, MPa	n_{H_2}/n_{HC}, mol·mol^{-1}	AY, % (by mass)	HAY, % (by mass)
N	522.1	521.3	522.6	524.0	0.88	3.5	66.85	22.60
A	520.0	520.0	523.8	528.6	0.80	3.0	67.63	22.57
B	523.1	527.5	523.8	529.3	0.85	3.6	66.79	20.76
C	520.2	520.6	524.5	528.6	0.83	3.4	67.20	21.71
D	521.5	521.0	523.8	529.3	0.88	3.6	67.03	20.83
E	523.1	522.0	530.0	530.0	0.90	4.0	66.17	19.51

archived genetic algorithm (NAGA), a Pareto-optimal set and several corresponding sets of decision variable values are obtained. The relations between each decision variable and the two objectives are also proposed and used for selecting the suitable solution from the Pareto set that is obtained. This multioptimization strategy will reduce the plant operation cost, improve the quality of products, and thereby increase the total profit. Moreover, the multioptimization method may also be applied to other industrial processes.

NOMENCLATURE

AY	aromatics yield, % (by mass)
$\boldsymbol{C}_p$	specific heat, kJ·kmol^{-1}·K^{-1}
E	activation energy, kJ·mol^{-1}
f_1, f_2	objective functions (f_1=K_f/AY, f_2=HAY/K_c, K_f=67, K_c=20)
H	height of the catalyst bed, m
ΔH	heat of reaction, kJ·kmol^{-1}
HAY	the yield of heavy aromatics, % (by mass)
K_r	matrix for the reaction rate coefficients
k	reaction rate coefficient, h^{-1}
k_0	frequency factor, s^{-1}·MPa$^{-\theta}$
LA	latent aromatics content of naphtha charge, % (by mass)
LHSV	liquid hourly space velocity, h^{-1}
n_{H_2} / n_{HC}	hydrogen-to-oil molar ratio, mol·mol^{-1}
p_h	partial pressure of hydrogen, MPa
p_r	reaction pressure, MPa
R	radius of the catalyst bed, m (or gas contant)
r	reaction rate, kmol·h^{-1}
T	reaction temperature, K
T_s	product separator temperature, ℃
T_1, T_2, T_3, T_4	four reactor inlet temperatures, ℃ (1—4 indicates the number of reactors)
V_c	catalyst volume, m^3
$\boldsymbol{Y}$	molar flow rate, kmol·h^{-1}
ϕ	catalyst deactivation factor

Superscripts

θ	pressure exponent

Subscripts

j	reaction number (j=1—31)

REFERENCES

1 Gao, Y., Shi, L., Yao, P.J., "Waste minimization through process integration and multi-objective optimization," *Chin. J. Chem. Eng.*, **9**(3), 267—272(2001).

2 Mu, S.J., Su, H.Y., Gu, Y., Chu, J., "Multi-objective optimization of industrial purified terephthalic acid oxidation process", *Chin. J. Chem. Eng.*, **11**(5), 536—541(2003).

3 Hou, W.F., Su, H.Y., Hu, Y.Y., Chu, J., "Simulation of industrial catalytic reforming process by development user's module on ASPEN PLUS platform", *J. Chem. Ind. Eng.*, **56**(9), 1714—1720(2005).

4 Li, S.J., Wang, H., Qian, F., "Multi-objective genetic algorithm and its applications in chemical engineering", *Comput. Appl. Chem.*, **20**(6), 755—760(2003). (in Chinese)

5 Yuen, C.C., Gupta, A., S.K., Ray, A.K., "Multi-objective optimization of membrane separation modules using genetic algorithm", *J. Membr. Sci.*, **176**, 177—196(2000).

6 Coello, C.C.A., "A short tutorial on evolutionary multiobjective optimization", In: Proceedings of the First International Conference on Evolutionary Multi-criterion Optimization, Zitzler, E., Deb, K., Thiele, L., Coello, C.C.A., Corne, D., Eds., Springer, Zurich, Switzerland, 67—81(2001).

7 Srinivas, N., Deb, K., "Multiobjective optimization using nondominated sorting in genetic algorithms", *Evol. Comput.*, **2**(3), 221—248(1994).

8 Horn, J., Nafpliotis, N., Goldberg, D.E., "A niched Pareto genetic algorithm for multiobjective optimization", In: Proceedings of the First IEEE Conference on Evolutionary Computation, IEEE World Congress on Computational Intelligence, IEEE Press, Piscata- way, New Jersey, **1**, 82—87(1994).

9 Knowles, J.D., Corne, D.W., "Approximating the nondominated front using Pareto archived evolution strategy", *Evol. Comput.*, **8**(2), 149—172(2000).

10 Zitzler, E., Thiele, L., "Multiobjective evolutionary algorithms: A comparative case study and the strength Pareto approach", *IEEE Trans. Evol. Comput.*, **3**(4), 257—271(1999).

11 Mu, S.J., Su, H.Y., Wang, Y.X., Chu, J., "An efficient evolutionary multi-objective optimization algorithm", In: Proceedings of the IEEE Congress on Evolutionary Computation, Canberra, **2**, 914—920(2003).

12 Mu, S.J., Su, H.Y., Jia, T., Gu, Y., Chu, J., "Scalable multi-objective optimization of industrial purified terephthalic acid (PTA) oxidation process", *Comput. Chem. Eng.*, **28**, 2219—2231(2004).

13 Hou, W.F., Su, H.Y., Hu, Y.Y., Chu, J., "A lumped kinetics model and its on-line application to a commercial catalytic naphtha reforming process", *J. Chem. Ind. Eng.*, **57**(7), 1605—1611(2006). (in Chinese)

14 Smith, R.B., "Kinetic analysis of naphtha reforming with platinum catalyst", *Chem. Eng. Progr.*, **55**(6), 76—80(1959).

15 Ramage, M.P., Graziani, K.R., Krambeck, F.J., "Development of Mobil's kinetic reforming model", *Chem. Eng. Sci.*, **35**, 41—48(1980).

16 Taskar, U., Riggs, J.B., "Modeling and optimization of a semiregenerative catalytic naphtha reformer", *AIChE J.*, **43**, 740—753(1997).

17 Rahimpour, M.R., Esmaili, S., Bagheri, G.N.A., "Kinetic and deactivation model for industrial catalytic naphtha reforming", *Iranian J. Sci. Tech., Trans. B: Tech.*, **27**, 279—290(2003).

18 Weng, H.X., Jiang, H.B., Chen, J., "Lumped model for catalytic reforming (Ⅱ) Experiment design and kinetic parameter estimation", *J. Chem. Ind. Eng.*, **45**(5), 531—537(1994). (in Chinese)

19 Xie, X.A., Peng, S.H., Liu, T.J., "Establishment and commercial application of kinetics models for catalytic reforming reactions (1) Establishment of physical model", *Petro. Ref. Eng.*, **25**(6), 49—51(1995). (in Chinese)

20 Zhou, Q.H., Hu, S.Y., Li, Y.R., Shen, J.Z., Wei, Z.W., "Molecular modeling and optimization for catalytic reforming", *Comput. Appl. Chem.*, **21**(3), 447—452(2004). (in Chinese)

21 Hou, W.F., Su, H.Y., Hu, Y.Y., Chu, J., "Modeling, simulation and optimization of a whole industrial catalytic naphtha reforming process on Aspen Plus platform", *Chin. J. Chem. Eng.*, **14**(5), 584—591(2006).